Characterization of a silicon-photonic multi-wavelength power monitor

Ryan Aguinaldo,[1,*] Peter O. Weigel,[1] Hannah Grant,[1] Christopher DeRose,[2] Anthony Lentine,[2] Andrew Pomerene,[2] Andrew Starbuck,[2] Douglas C. Trotter,[2] and Shayan Mookherjea[1,*]

[1] *University of California, San Diego, Mail Code 0407, La Jolla, California 92093-0407 USA*

[2] *Sandia National Laboratories, Applied Photonic Microsystems, Albuquerque, New Mexico 87185 USA*

**Email: raguinaldo@ucsd.edu, smookherjea@ucsd.edu*

***Abstract*—We describe the design and operation of a silicon-photonic device for monitoring power variations of individual channels in a multi-wavelength DWDM network. Amplitude variations of ~20 dB, for channels spaced by 100 GHz, are measured.**

The University of California, San Diego MORDIA (Microsecond Optical Reconfigurable Datacenter Interconnect Architecture [1]) DWDM ring network supports up to 24 wavelength channels, each carrying 10-Gbps data. The transceivers (one for each channel) in MORDIA are commercial DWDM SFP+ form-factor modules, which are aligned on the ITU-T 100-GHz communications grid. A conventional optical spectrum analyzer (OSA) is used to read the optical power levels of each channel. Since these sources are of known center frequencies and lineshapes, the main utility of the OSA is the ability to track intensity changes in each of the known channels. We have designed a silicon-photonic device that provides the same needed information with many orders-of-magnitude reduction in size, weight, and power. Our on-chip solution, which is based on cascaded-microring filters [2], also offers the opportunity for monolithic integration with other silicon photonic components and subsystems.

The silicon-photonic chip was fabricated at Sandia National Laboratories on 200-mm SOI wafers (230-nm Si thickness) as part of the CIAN-Sandia collaboration. As shown in Fig. 1a, our chip-scale architecture consists of a 24-element filter bank in which each filtering section consists of a 7^{th}-order microring drop filter, weakly coupled to the bus waveguide (a total of 168 microrings are used). As shown in Fig. 1b, the center wavelengths of each filter are approximately graded with a filter-to-filter passband center spacing of ~0.4 nm. The drop bandwidth of the filters (defined by the magnitude of the coupling coefficient between the microrings) is measured to be ~2 nm. The bandwidth was intentionally greater than the channel-to-channel spacing, so that multiple detector readouts are obtained for each wavelength. Dithering, via imperfect apodization of the rings, is useful to obtain non-identical detector readouts for wavelengths in close proximity to each other (e.g., separated by less than the passband width). The microrings consist of waveguides that are adiabatically widened in two sections, with an implanted inner section, so that they can be thermally

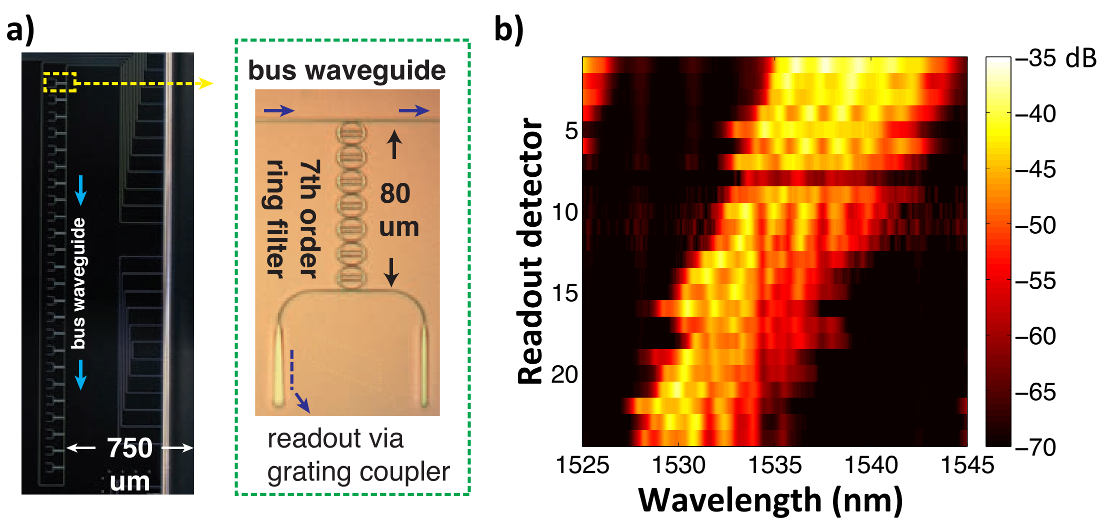

Fig. 1. a) Chip-scale multi-wavelength power monitor; dark-field micrograph of the 24-element filter bank. The inset shows one of the 24 drop-filters, consisting of seven cascaded microrings. **b)** Transmission spectra of the 24 filters (i.e. readout detectors).

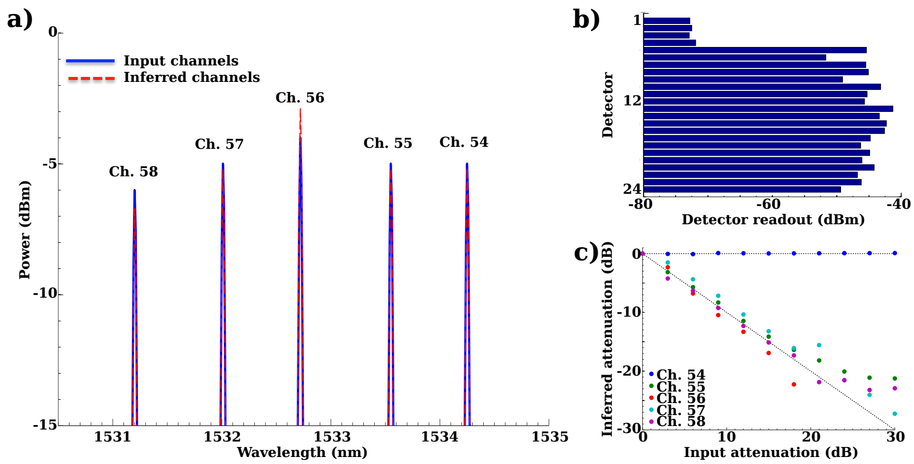

Fig. 2. a) Input and inferred (i.e. reconstructed) spectra. The power in the laser lines, labeled by their ITU channels, form the elements of vector **P**. **b)** Detector readouts corresponding to the input spectrum in (a); these form the elements of vector **D**. **c)** The inferred attenuation of the present channels when the power of Ch. 54 is held constant and Ch. 55-58 are attenuated by the same amounts. The horizontal and sloped dotted lines show the ideal behavior for the constant and attenuated channels, respectively.

tuned, if necessary; however, no thermal tuning was needed for the results shown here. A higher-order microring filter was used because a single microring has a relatively broad Lorentzian lineshape, which would cause inter-channel crosstalk and degrade the transmitted light in the bus waveguide after only a few stages.

The 24 filters each drop their signals to 24 corresponding detection ports, which are grating couplers on a 125-µm pitch. For testing purposes, the signals from the gratings were individually coupled to a lensed fiber and detected with a high-sensitivity InGaAs photdoiode. We also coupled the grating signals to an InGaAs sensor array, via a microscope, for the purpose of simultaneous readout. Both methods yielded similar information for a narrow-band tunable-laser input signal.

An arbitrary, but unknown, power distribution can be represented by the column vector **P**; each element of **P** corresponds to a single wavelength channel in the network. When this power distribution propagates through the device, power is routed to the 24 detection ports via the transmission spectra. These detector readouts can be represented by the 24-element column vector $\mathbf{D} = \mathbf{V} \times \mathbf{P}$, where **V** is a $24 \times n$ matrix and n is the number of data channels (wavelengths) present in the network. **V** is measured as part of the initial device characterization. During real-time operation, **D** is measured and P is estimated as $\mathbf{P} = \mathbf{V}^{-1} \times \mathbf{D}$, where the Moore-Penrose pseuoinverse $\mathbf{V}^{-1}$ provides the unique optimal solution in the least-squares sense, provided that $n \leq 24$. This condition ensures that **V** is of full-column rank and that its left inverse exists [3].

Figure 2 shows an example of a five-channel reconstruction, using laser sources corresponding to ITU Channels 54-58. The input channels in Fig. 2.a compose the unknown **P**, which is the reconstruction goal of the algorithm. The corresponding detector readouts of **D** are plotted in Fig. 2b. Solving the inverse problem yields the inferred (i.e., reconstructed) power levels of the five channels, as plotted in Fig. 2a. Good agreement is observed with the original input. Next, we gradually attenuate the power levels of channels 55 to 58 while keeping the power level of channel 54 constant. At present, our device is able to track these power changes over about 20 dB of dynamic range. We attribute errors in the reconstruction to input amplitude variations, which can occur due to the slow measurement process of accessing the 24 grating couplers one-at-a-time via lensed fiber. Further improvements are expected in the next chip version by coupling the detection ports to on-chip integrated photodetectors, which can provide for simultaneous electronic readout of the 24 detection ports.

The authors are grateful to the CIAN ERC EEC-0812072 and NSF MRI ECCS 1229677. Sandia is a multiprogram laboratory operated by Sandia Corporation, a Lockheed Martin Company, for the United States Department of Energy's National Nuclear Security Administration under contract DE-AC04-94AL85000.

[1] N. Farrington et al., *Photon. Technol. Lett.* **25**, 1589 (2013).

[2] J.R. Ong, R. Kumar and S. Mookherjea, *Photon. Technol. Lett.* **25**, 1543 (2013).

[3] R.A. Horn and C.R. Johnson, *Matrix Analysis* (Cambridge University Press, Cambridge, UK, 1985).